



Article

Incorporation of Hexanuclear Mn(II,III) Carboxylate Clusters with a $\{Mn_6O_2\}$ Core in Polymeric Structures

Mariana Darii ¹, Irina G. Filippova ¹, Jürg Hauser ², Silvio Decurtins ², Shi-Xia Liu ² , Victor Ch. Kravtsov ^{1,*}  and Svetlana G. Baca ¹ 

¹ Institute of Applied Physics, Academy of Sciences of Moldova, Academiei 5, MD-2028 Chisinau, Moldova; mariana.darii@mail.ru (M.D.); irina.filippova@phys.asm.md (I.G.F.); sbaca_md@yahoo.com (S.G.B)

² Departement für Chemie und Biochemie, Universität Bern, Freiestrasse 3, 3012-Bern, Switzerland; juerg.hauser@krist.unibe.ch (J.H.); silvio.decurtins@dcb.unibe.ch (S.D.); shi-xia.liu@dcb.unibe.ch (S.-X.L.)

* Correspondence: kravtsov@phys.asm.md; Tel.: +373-22-738-154

Received: 11 January 2018; Accepted: 15 February 2018; Published: 17 February 2018

Abstract: A new series of hexanuclear mixed-valent carboxylate coordination clusters of the type $[Mn_6O_2(O_2CR)_{10}L_4]$ ($R = CMe_3$; $CHMe_2$) featuring a $\{Mn^{II}_4Mn^{III}_2(\mu_4-O)_2\}$ core of composition $[Mn_6O_2(O_2CCMe_3)_{10}(Me_3CCO_2H)_3(EtOH)] \cdot (Me_3CCO_2H)$ (**1**), $[Mn_6O_2(O_2CCMe_3)_{10}(Me_3CCO_2H)_2(EtOH)_2] \cdot 2(EtOH)$ (**2**) and $[Mn_6O_2(O_2CCMe_3)_{10}(Me_3CCO_2H)_2(MeOH)_2] \cdot 2(MeOH) \cdot H_2O$ (**3**), and coordination polymers which incorporate such clusters, namely $[Mn_6O_2(O_2CCHMe_2)_{10}(pyz)(MeOH)_2]_n$ (**4**), $\{[Mn_6O_2(O_2CCHMe_2)_{10}(pyz)_{1.5}(H_2O)] \cdot 0.5(H_2O)\}_n$ (**5**), and $[Mn_6O_2(O_2CCMe_3)_{10}(HO_2CCMe_3)_2(en)]_n$ (**6**), have been synthesized (where *pyz* = pyrazine, *en* = ethyl nicotinate). The modification of the cluster surface by a diverse combination of capped or bridging ligands attached to peripheral Mn^{II} atoms results in discrete clusters with a closed hydrophobic exterior shell in **1** and **2**, supramolecular chains built through hydrogen bonded solvent molecule clusters in **3**, linear coordination polymers in **4** and **6** or a ladder-like coordination polymer in **5**. The H-bonded coordination polymers **4** and **5** form supramolecular layers in crystals.

Keywords: manganese cluster; cluster-based coordination polymer; X-ray diffraction analysis

1. Introduction

Hexanuclear Mn(II,III) carboxylate clusters with a mixed valent $\{Mn^{II}_4Mn^{III}_2(\mu_4-O)_2\}$ core have been successfully used as building blocks for the synthesis of cluster-based coordination polymers (CCPs) [1] starting from the first prepared CCP by Yamashita et al. in 2002 [2]. This type of cluster has a common formula $[Mn_6O_2(O_2CR)_{10}L_4]$ (where *L* = monodentate neutral ligand) is stable and able to resist decomposition during the reaction and may introduce its inherent physical properties in newly formed structures. Moreover, in the hexanuclear oxo-carboxylate Mn(II,III) clusters, various capped monodentate neutral ligands *L* may be obtained and completely or partially replaced by bridging ligands to give coordination polymers. Furthermore, under specific conditions, the role of carboxylate ligands can be changed from intracluster bridges to intercluster bridges with the formation of polymeric structures. Such structures are characterized by short distances between nearest $\{Mn_6\}$ clusters: the closest intercluster Mn...Mn distances of 4.79 and 4.88 Å have been reported for acetato-bridged $\{[Mn_6O_2(O_2CMe)_{10}(H_2O)_4] \cdot 2.5(H_2O)\}_n$ [3] and for propionate-bridged $\{[Mn_6O_2(O_2CEt)_{10}(H_2O)_4] \cdot 2(EtCO_2H)\}_n$ [4] CCPs, respectively. Notably, the choice of exo-polydentate spacer ligands, selection of precursors and reaction conditions make it possible to obtain CCPs that incorporate hexanuclear Mn(II,III) clusters with different dimensionality—1D polymeric chains [2–6], 2D layers [7,8] and 3D networks [9]. The spacer length and spacer flexibility both have an important effect on the complex structure and physical

properties of the end-product. For example, the replacement of one pivalic acid molecule in $[\text{Mn}_6\text{O}_2(\text{O}_2\text{CCMe}_3)_{10}(\text{Me}_3\text{CCO}_2\text{H})_4]$ by a long 4,4'-bipyridine ligand leads to the organization of a 1D zigzag polymeric chain with $\text{Mn}\cdots\text{Mn}$ intercluster distances of 11.68 Å [2]. Nearly linear chains are also formed by bridged nicotinamide molecules which are coordinated through an amid O atom and a pyridine N atom ($\text{Mn}\cdots\text{Mn}$ distance is 8.690 Å) [5]. Unique meander-type chains are formed in $\{[\text{Mn}_6\text{O}_2(\text{O}_2\text{CCHMe}_2)_{10}(\text{Me}_2\text{CHCO}_2)(\text{EtOH})(\text{bpe})]\cdot\text{Me}_2\text{CHCO}_2\}_n$ where the hexanuclear $\{\text{Mn}_6\}$ clusters are linked by 1,2-bis(4-pyridyl)ethane (bpe) ($\text{Mn}\cdots\text{Mn}$ distance is 9.239 Å) [5]. The shorter rigid pyrazine (pyz) ligand connects neighboring clusters in $\{[\text{Mn}_6\text{O}_2(\text{O}_2\text{CCHMe}_2)_{10}(\text{pyz})_3]\cdot\text{H}_2\text{O}\}_n$ into a zigzag chain with $\text{Mn}\cdots\text{Mn}$ distances of 7.222 Å [5]. Pyrazine molecules occupy four sites in peripheral Mn^{II} centers, but two of them serve as exo-bidentate ligands, while two others are monodentate. As can be seen from the given examples, despite the potential for cross-linking into 2D or 3D networks, the employed spacer ligands resulted exclusively in 1D polymer chains that are packed in parallel or both parallel and perpendicular propagation directions in the crystal.

The first reported 2D coordination polymers based on hexanuclear $\{\text{Mn}_6\}$ carboxylate clusters were prepared using isonicotinamid (ina) as an N,O-donor bridging ligand [7]. In this case, all four capped molecules in the initial $\{\text{Mn}_6\}$ cluster have been substituted by ina that led to the formation of two-dimensional (4,4) layers in $\{[\text{Mn}_6\text{O}_2(\text{O}_2\text{CCMe}_3)_{10}(\text{ina})_2]\cdot 2(\text{EtOAc})\}_n$. Using the same spacer, a solvent free $[\text{Mn}_6\text{O}_2(\text{O}_2\text{CCMe}_3)_{10}(\text{ina})_2]_n$ 2D coordination polymer has also been obtained [8]. Two different 2D CCPs $\{[\text{Mn}_6\text{O}_2(\text{O}_2\text{CCMe}_3)_{10}(\text{adt})_2]\cdot 2(\text{thf})\}_n$ and $\{[\text{Mn}_6\text{O}_2(\text{O}_2\text{CCHMe}_2)_{10}(\text{adt})_2]\cdot (\text{thf})\cdot 3(\text{EtOH})\}_n$ were synthesized utilizing the angled semi-rigid N,N'-donor aldrithiol spacer (adt) [8]. In the first of them, each Mn_6 cluster is connected via adt ligands to four neighbors in 2D networks with a (4,4) topology similar to the above-mentioned CCP with isonicotinamide ligand, whereas in the second case an unprecedented 2D bilayer motif is formed. Examples of 3D oxo-hexanuclear CCPs are very rare with only two CCPs, $[\text{Mn}_6\text{O}_2(\text{O}_2\text{CCMe}_3)_{10}(\text{NIT-Me})_2]_n$ [6] and $[\text{Mn}_6\text{O}_2(\text{O}_2\text{CCH}_2\text{C}_6\text{H}_5)_{10}(\text{pyz})_2]_n$ [9], that have been prepared using a stable nitronyl nitroxide radical 2,4,4,5,5-pentamethyl-4,5-dihydro-1H-imidazolyl-3-oxide-1-oxyl (NIT-Me) or pyrazine, respectively.

It should be noted that hexanuclear $\text{Mn}(\text{II,III})$ carboxylate clusters based on pivalate or isobutyrate ligands represent globe-shaped nanosized particles with *ca.* $2.0 \times 1.8 \times 1.5$ nm dimension with a hydrophobic surface and which are malleable for modification. The methylene groups of the ligands on the surface of such clusters are often disordered and crystal solvent molecules may be incorporated. The disorder is manifested as being essentially enhanced compared with the cluster core thermal motion or resolved with two different positions of disordered fragments. Such a labile cluster surface allows to accommodate different combinations of capped or bridging ligands and solvent molecules; however, this complicates the prediction of a final cluster composition and cluster-based polymer topology. In continuation of our study on the design and preparation of cluster-based coordination polymeric networks based on $\text{Mn}(\text{II, III})$ carboxylate clusters, here we report the syntheses and the crystal structures of a new series of compounds containing a stable $[\text{Mn}_6\text{O}_2(\text{O}_2\text{CR})_{10}]$ core: discrete hexanuclear clusters $[\text{Mn}_6\text{O}_2(\text{O}_2\text{CCMe}_3)_{10}(\text{Me}_3\text{CCO}_2\text{H})_3(\text{EtOH})]\cdot(\text{Me}_3\text{CCO}_2\text{H})$ (1), $[\text{Mn}_6\text{O}_2(\text{O}_2\text{CCMe}_3)_{10}(\text{Me}_3\text{CCO}_2\text{H})_2(\text{EtOH})_2]\cdot 2(\text{EtOH})$ (2) $[\text{Mn}_6\text{O}_2(\text{O}_2\text{CCMe}_3)_{10}(\text{Me}_3\text{CCO}_2\text{H})_2(\text{MeOH})_2]\cdot 2(\text{MeOH})\cdot\text{H}_2\text{O}$ (3), and 1D cluster-based coordination polymers $[\text{Mn}_6\text{O}_2(\text{O}_2\text{CCHMe}_2)_{10}(\text{pyz})(\text{MeOH})_2]_n$ (4), $\{[\text{Mn}_6\text{O}_2(\text{O}_2\text{CCHMe}_2)_{10}(\text{pyz})_{1.5}(\text{H}_2\text{O})]\cdot 0.5(\text{H}_2\text{O})\}_n$ (5), and $[\text{Mn}_6\text{O}_2(\text{O}_2\text{CCMe}_3)_{10}(\text{HO}_2\text{CCMe}_3)_2(\text{en})]_n$ (6), where $\{\text{Mn}_6\}$ clusters are arranged by pyrazine (pyz) or ethyl nicotinate (en) into linear (4 and 6) and ladder-like (5) chains.

2. Experimental Section

2.1. Materials and Methods

All manipulations were performed under aerobic conditions using chemicals and solvents as received without further purification. The precursors $\text{Mn}(\text{Me}_3\text{CCO}_2)_2$, $\text{Mn}(\text{Me}_2\text{CHCO}_2)_2$ have been prepared by using methods described elsewhere [10,11]. Cluster $[\text{Mn}_6\text{O}_2(\text{O}_2\text{CCMe}_3)_{10}(\text{Me}_3\text{CCO}_2\text{H})_4]$ has been prepared with a slight modification [11] by the reaction of manganese(II) acetate with an excess of pivalic acid followed by adding MeCN solution to the reaction mixture. Recrystallization of the precipitated solid from hot tetrahydrofuran yields $[\text{Mn}_6(\text{O}_2\text{CCMe}_3)_{10}(\text{thf})_4]$ [12]. IR spectra were recorded in the solid state on a Perkin-Elmer Spectrum 100 FT-IR (Perkin-Elmer, Waltham, MA, USA) spectrometer in the $650\text{--}4000\text{ cm}^{-1}$ range.

2.2. X-ray Crystallography

Diffraction datasets were collected on a SuperNova diffractometer (for **1**, **3**, and **6**, Rigaku, Tokyo, Japan), Bruker APEX II (for **5**, Bruker AXS Inc., Madison, WI, USA), and Xcalibur E (for **2** and **4**, Oxford diffraction LTD., Yarnton, UK) CCD area-detector diffractometers using mirror optics or graphite monochromated Mo-K α radiation. The crystallographic data and summary of the data collection and refinement are listed in Table 1. Data were corrected for Lorentz, polarization effects, and absorption. The structures were solved by direct methods and refined by full-matrix least squares on weighted F^2 using the SHELX suite of programs [13]. In all structures, *tert*-butyl and isopropyl groups show enhanced thermal motion. The hydrogen atoms were placed in calculated, ideal positions and refined as riding on their respective atoms. The hydrogen atoms of disordered solvent molecules have not been localized or included in the model of refinement.

2.3. Synthesis

Synthesis of $[\text{Mn}_6\text{O}_2(\text{O}_2\text{CCMe}_3)_{10}(\text{HO}_2\text{CCMe}_3)_3(\text{EtOH})] \cdot (\text{Me}_3\text{CCO}_2\text{H})$ (**1**). $\text{Mn}(\text{Me}_3\text{CCO}_2)_2$ (0.16 g, 0.622 mmol) and triethanolamine (H_3tea) (0.02 g, 0.144 mmol) were dissolved in an EtOH/ CH_2Cl_2 mixture (5 mL/5 mL). The resulting brown solution was heated under reflux for 30 min and then filtered. The filtrate was allowed to slowly evaporate in a vial covered with a plastic cap. Brown crystals suitable for X-ray measurements were obtained in a week, washed with EtOH and dried in air. Yield (based on Mn): 0.051 g, 27%. Elemental analyses calcd. for $\text{C}_{72}\text{H}_{136}\text{Mn}_6\text{O}_{31}$ (1827.44 g mol $^{-1}$): C 47.32, H 7.50; found: C 47.26, H 7.27%. IR (ν , cm^{-1}): 3676 w, 2961 m, 2926 sh, 2902 sh, 1693 w, 1578 sh, 1565 v/s, 1481 m, 1459 m, 1408 v/s, 1374 s, 1358 s, 1318 w, 1225 s, 1207 sh, 1066 m, 1048 m, 938 w, 894 m, 872 w, 787 m. Compound **1** can also be prepared by dissolving of $[\text{Mn}_6\text{O}_2(\text{O}_2\text{CCMe}_3)_{10}(\text{Me}_3\text{CCO}_2\text{H})_4]$ (0.18 g, 0.101 mmol) in hot CH_2Cl_2 (5 mL) followed by adding EtOH (5 mL) with two drops of H_3tea . Identity has been confirmed by its IR spectrum and the measurement of a single crystal with an identical unit cell.

Synthesis of $[\text{Mn}_6\text{O}_2(\text{O}_2\text{CCMe}_3)_{10}(\text{HO}_2\text{CCMe}_3)_2(\text{EtOH})_2] \cdot 2(\text{EtOH})$ (**2**). $\text{Mn}(\text{Me}_3\text{CCO}_2)_2$ (0.16 g, 0.622 mmol), $\text{La}(\text{NO}_3)_3 \cdot 6\text{H}_2\text{O}$ (0.03 g, 0.215 mmol) and triethanolamine (H_3tea) (0.02 g, 0.144 mmol) were dissolved in an EtOH/MeCN mixture (5 mL/5 mL). The resulting brown solution was heated under reflux for 30 min and then filtered. The filtrate was allowed to slowly evaporate in a vial covered with a plastic cap. Brown crystals suitable for X-ray measurements were obtained in a week, washed with EtOH and dried in air. Yield (based on Mn): 0.020 g, 40%. IR (ν , cm^{-1}): 3676 w, 2960 m, 2928 sh, 2902 sh, 1694 w, 1584 sh, 1567 v/s, 1481 m, 1412 m, 1374 s, 1358 v/s, 1225 s, 1207 sh, 1066 m, 1045 m, 937 w, 894 m, 873 w, 786 m, 763 w.

Table 1. Crystal data and details on the structure refinement for 1–6.

	1	2	3	4	5	6
Empirical formula	C ₇₂ H ₁₃₆ Mn ₆ O ₃₁	C ₆₈ H ₁₃₄ Mn ₆ O ₃₀	C ₆₄ H ₁₂₈ Mn ₆ O ₃₁	C ₄₆ H ₈₂ Mn ₆ N ₂ O ₂₄	C ₉₂ H ₁₅₈ Mn ₁₂ N ₆ O ₄₇	C ₆₈ H ₁₁₉ Mn ₆ NO ₂₈
<i>M_r</i> (g mol ^{−1})	1827.44	1761.38	1723.3	1376.77	2759.53	1728.27
<i>T</i> (K)	150(2)	293(2)	173(2)	293(2)	296(2)	150(2)
Crystal system	Triclinic	Monoclinic	Monoclinic	Triclinic	Triclinic	Monoclinic
Space group	<i>P</i> -1	<i>C</i> 2/ <i>c</i>	<i>P</i> 2 ₁ / <i>n</i>	<i>P</i> -1	<i>P</i> -1	<i>Cc</i>
<i>a</i> (Å)	13.4165(2)	13.4037(5)	14.6642(1)	13.1919(9)	12.7175(6)	24.9206(3)
<i>b</i> (Å)	15.7141(2)	29.2459(11)	22.9974(2)	13.3591(7)	13.3257(6)	14.3552(2)
<i>c</i> (Å)	25.3229(3)	23.7135(11)	25.9750(2)	20.8662(9)	21.8431(10)	26.5404(4)
<i>α</i> (°)	73.080(1)	90	90	100.647(4)	72.388(1)	90
<i>β</i> (°)	79.534(1)	88.703(4)	100.022(1)	93.502(4)	81.217(1)	115.847(2)
<i>γ</i> (°)	66.796(1)	90	90	112.826(6)	66.346(1)	90
<i>V</i> (Å ³)	4680.9(1)	9293.4(7)	8626.1(1)	3295.0(3)	3229.7(3)	8544.7(2)
<i>Z</i> , <i>ρ</i> (Mg m ^{−3})	2, 1.297	4, 1.259	4, 1.327	2, 1.388	1, 1.419	4, 1.343
<i>μ</i> (mm ^{−1})	0.856	0.859	0.925	1.185	1.209	0.932
<i>F</i> (000)	1932	3728	3640	1428	1428	3632
Crystal size (mm)	0.34 × 0.24 × 0.15	0.60 × 0.40 × 0.12	0.28 × 0.25 × 0.09	0.60 × 0.25 × 0.10	0.16 × 0.16 × 0.08	0.13 × 0.10 × 0.05
<i>θ</i> range (°)	1.453–28.235	2.930–24.999	1.592–24.999	3.105–24.500	1.731–25.000	1.684 to 25.999
Index ranges	−17 ≤ <i>h</i> ≤ 17,	−15 ≤ <i>h</i> ≤ 15,	−17 ≤ <i>h</i> ≤ 17,	−15 ≤ <i>h</i> ≤ 15,	−15 ≤ <i>h</i> ≤ 15,	−30 ≤ <i>h</i> ≤ 30,
	−20 ≤ <i>k</i> ≤ 20,	−34 ≤ <i>k</i> ≤ 34,	−27 ≤ <i>k</i> ≤ 27,	−15 ≤ <i>k</i> ≤ 14,	−15 ≤ <i>k</i> ≤ 15,	−17 ≤ <i>k</i> ≤ 17,
	−33 ≤ <i>l</i> ≤ 33	−28 ≤ <i>l</i> ≤ 26	−30 ≤ <i>l</i> ≤ 30	−24 ≤ <i>l</i> ≤ 24	−25 ≤ <i>l</i> ≤ 25	−32 ≤ <i>l</i> ≤ 32
Reflections	200157/21845	26421/8169	91815/15189	19693/10877	25957/11303	66940/16778
collected/unique	[<i>R</i> _{int} = 0.0431]	[<i>R</i> _{int} = 0.0510]	[<i>R</i> _{int} = 0.0317]	[<i>R</i> _{int} = 0.0456]	[<i>R</i> _{int} = 0.0441]	[<i>R</i> _{int} = 0.0748]
Completeness to <i>θ</i> _{max}	99.8%	99.8%	99.9%	99.1%	99.6%	100%
Data /restraints/ parameters	21845 / 0 / 989	8169 / 80 / 520	15189 / 92 / 966	10877 / 13 / 748	11303 / 3 / 720	16778 / 60 / 939
Final <i>R</i> indices [<i>I</i> > 2σ(<i>I</i>)]	<i>R</i> ₁ = 0.0401,	<i>R</i> ₁ = 0.0651	<i>R</i> ₁ = 0.0463,	<i>R</i> ₁ = 0.0848	<i>R</i> ₁ = 0.0416,	<i>R</i> ₁ = 0.0508,
	<i>wR</i> ₂ = 0.0988	<i>wR</i> ₂ = 0.1727	<i>wR</i> ₂ = 0.1290	<i>wR</i> ₂ = 0.2247	<i>wR</i> ₂ = 0.0934	<i>wR</i> ₂ = 0.987
<i>R</i> indices (all data)	<i>R</i> ₁ = 0.0522,	<i>R</i> ₁ = 0.1043	<i>R</i> ₁ = 0.0555,	<i>R</i> ₁ = 0.1264,	<i>R</i> ₁ = 0.0704,	<i>R</i> ₁ = 0.0757,
	<i>wR</i> ₂ = 0.1073	<i>wR</i> ₂ = 0.1979	<i>wR</i> ₂ = 0.1354	<i>wR</i> ₂ = 0.2581	<i>wR</i> ₂ = 0.1022	<i>wR</i> ₂ = 0.1096
Goodness-of-fit on <i>F</i> ²	1.007	1.007	1.008	1.016	1.003	1.007
Largest diff. peak and hole (e Å ^{−3})	1.264 and −0.663	0.456 and −0.392	1.133 and −0.668	1.652 and −0.664	1.210 and −0.437	0.415 and −0.332

Crystallographic data for the structural analysis have been deposited with the Cambridge Crystallographic Data Centre, CCDC Nos. 1815847 for **1**, 1815848 for **2**, 1815849 for **3**, 1815850 for **4**, 1815851 for **5**, and 1815852 for **6**. Copies of the data can be obtained free of charge from the Cambridge Crystallographic Data Centre, 12 Union Road, Cambridge CB2 1EZ, UK (Fax: +44-1223-336-033; e-mail: deposit@ccdc.cam.ac.uk).

Synthesis of $[\text{Mn}_6\text{O}_2(\text{O}_2\text{CCMe}_3)_{10}(\text{HO}_2\text{CCMe}_3)_2(\text{MeOH})_2] \cdot 2(\text{MeOH}) \cdot \text{H}_2\text{O}$ (3). $[\text{Mn}_6\text{O}_2(\text{O}_2\text{CCMe}_3)_{10}(\text{Me}_3\text{CCO}_2\text{H})_4]$ (0.3 g, 0.168 mmol), $\text{Dy}(\text{NO}_3)_3 \cdot 6\text{H}_2\text{O}$ (0.01 g, 0.028 mmol) and triethanolamine (H_3tea) (0.004 g, 0.0268 mmol) were dissolved in a $\text{MeOH}/\text{CH}_2\text{Cl}_2$ (5 mL/5 mL) mixture. The reaction mixture was treated in an ultrasonic bath for 40 min. The dark-brown solution was filtered and allowed to evaporate slowly at room temperature. Brown crystals suitable for X-ray measurements were obtained in one week and washed with MeOH and dried in air. Yield (based on Mn): 0.015 g, 53%. Elemental analyses calcd. for $\text{C}_{64}\text{H}_{128}\text{Mn}_6\text{O}_{31}$ ($1723.3 \text{ g mol}^{-1}$): C 43.03, H 6.87; found: C 42.61, H 6.87%. IR (ν , cm^{-1}): 3676 w, 2971 m, 2928 sh, 2902 sh, 1694 w, 1579 sh, 1566 v/s, 1482 m, 1458 m, 1409 v/s, 1374 s, 1359 s, 1312 w, 1225 s, 1205 sh, 1074 sh, 1066 m, 1057 m, 938 w, 894 m, 872 w, 787 m.

Synthesis of $[\text{Mn}_6\text{O}_2(\text{O}_2\text{CCHMe}_2)_{10}(\text{pyz})(\text{MeOH})_2]_n$ (4). $\text{Mn}(\text{Me}_2\text{CHCO}_2)_2$ (0.1 g, 0.436 mmol), [bis(2-hydroxyethyl)amino]acetonitrile hydrochloride (0.13 g, 0.725 mmol) and pyrazine (0.03 g, 0.375 mmol) were dissolved in a MeCN/MeOH (4 mL/4 mL) mixture. The reaction mixture was treated in ultrasonic bath for 30 minutes and then filtered. The filtrate was kept in a closed vial at room temperature. After one week, orange crystals suitable for single-crystal X-ray analysis were filtered off, washed with MeCN and dried in air. Yield (based on Mn): 0.0267 g, 27%. Elemental analyses calcd. for $\text{C}_{46}\text{H}_{77}\text{Mn}_6\text{N}_2\text{O}_{24}$ ($1371.73 \text{ g mol}^{-1}$): C 40.27, H 5.65, N 2.04; found: C 38.90, H 5.77, N 1.97%. IR (ν , cm^{-1}): 3661 w, 2971 s, 2927 sh, 2902 sh, 1578 s, 1469 m, 1413 v/s, 1370 m, 1294 m, 1251 m, 1089 sh, 1079 s, 1067 s, 1057 sh, 1044 s, 926 w, 892 w, 841 m, 798 w, 779 w, 763 w.

Synthesis of $\{[\text{Mn}_6\text{O}_2(\text{O}_2\text{CCHMe}_2)_{10}(\text{pyz})_{1.5}(\text{H}_2\text{O})] \cdot 0.5(\text{H}_2\text{O})\}_n$ (5). $\text{Mn}(\text{Me}_2\text{CHCO}_2)_2$ (0.03 g, 0.131 mmol), pyrazine (pyz) (0.01 g, 0.125 mmol) and 2-hydroxy-5-methoxy-3-nitrobenzaldehyde (0.025 g, 0.127 mmol) were dissolved in MeCN (8 mL). The resulting orange solution was heated under reflux for 30 min and then filtered. The filtrate was allowed to slowly evaporate in a vial covered with a plastic cap. The obtained reddish-brown crystals of 5 suitable for X-ray measurements were obtained in a month, washed with MeCN and dried in air. Yield (based on Mn): 0.0051 g, 17%. IR (ν , cm^{-1}): 3063 br/m, 2924 m, 2872 m, 2855 m, 1579 v/s, 1541sh, 1419 v/s, 1358v/s, 1287 s, 1247 m, 1218 sh, 1135 sh, 1093 sh, 1045 m, 934 w, 874 w, 815 m, 775 s, 741 w, 695 w.

Synthesis of $[\text{Mn}_6\text{O}_2(\text{O}_2\text{CCMe}_3)_{10}(\text{HO}_2\text{CCMe}_3)_2(\text{en})]_n$ (6). The mixture of $[\text{Mn}_6\text{O}_2(\text{O}_2\text{CCMe}_3)_{10}(\text{thf})_4]$ (0.1 g, 0.061 mmol) and ethyl nicotinate (0.03 g, 0.198 mmol) in decane (5 mL) was stirred in an open flask for 10 minutes at the temperature of 170°C . Afterwards, it was filtered and kept open until the red-brownish crystals were formed. The crystals of 6, suitable for single-crystal X-ray analysis, were filtered off, washed with MeCN and dried in air. Yield: 0.07 g, 68%. Elemental analyses calcd. for $\text{C}_{68}\text{H}_{119}\text{Mn}_6\text{NO}_{28}$ ($1728.27 \text{ g mol}^{-1}$): C, 47.26; H, 6.94; N, 0.81; found: C, 47.67; H, 7.87; N, 1.01%.

3. Results and Discussion

3.1. Synthetic Aspects

The variation of solvent media for simple manganese pivalate salt led to the formation of hexanuclear compounds with stable $[\text{Mn}_6\text{O}_2(\text{O}_2\text{CCMe}_3)_{10}]$ units while comprising different coordinated neutral monodentate ligands: three pivalic and one ethanol molecules in $[\text{Mn}_6\text{O}_2(\text{O}_2\text{CCMe}_3)_{10}(\text{Me}_3\text{CCO}_2\text{H})_3(\text{EtOH})] \cdot (\text{Me}_3\text{CCO}_2\text{H})$ (1) or two pivalic and two ethanol molecules in $[\text{Mn}_6\text{O}_2(\text{O}_2\text{CCMe}_3)_{10}(\text{Me}_3\text{CCO}_2\text{H})_2(\text{EtOH})_2] \cdot 2(\text{EtOH})$ (2) when $\text{EtOH}/\text{CH}_2\text{Cl}_2$ or EtOH/MeCN solution was used. Moreover, two pivalic acids and two methanol molecules in $[\text{Mn}_6\text{O}_2(\text{O}_2\text{CCMe}_3)_{10}(\text{Me}_3\text{CCO}_2\text{H})_2(\text{MeOH})_2] \cdot 2(\text{MeOH}) \cdot \text{H}_2\text{O}$ (3) were coordinated when a $\text{MeOH}/\text{CH}_2\text{Cl}_2$ mixture was utilized, Figure S1. The use of some amount of lanthanide salts in the synthesis of 2 and 3 was mandatory and afforded crystals 2–3 suitable for single-crystal X-ray measurements. The reaction of manganese isobutyrate with pyrazine spacer in the presence of [bis(2-hydroxyethyl)amino]acetonitrile hydrochloride in MeOH/MeCN afforded the linear cluster-based coordination polymer

$[\text{Mn}_6\text{O}_2(\text{O}_2\text{CCHMe}_2)_{10}(\text{pyz})(\text{MeOH})_2]_n$ (**4**) with a good yield of 40%. Using in the similar reaction 2-hydroxy-5-methoxy-3-nitrobenzaldehyde instead of the amino-acetonitrile derivative in MeCN gave the ladder-like CCP $[\text{Mn}_6\text{O}_2(\text{O}_2\text{CCHMe}_2)_{10}(\text{pyz})_{1.5}(\text{H}_2\text{O})] \cdot 0.5(\text{H}_2\text{O})_n$ (**5**) with 17% yield. The reaction of $[\text{Mn}_6\text{O}_2(\text{O}_2\text{CCMe}_3)_{10}(\text{thf})_4]$ pivalate cluster with ethyl nicotinate in decane led to the linear $[\text{Mn}_6\text{O}_2(\text{O}_2\text{CCMe}_3)_{10}(\text{HO}_2\text{CCMe}_3)_2(\text{en})]_n$ (**6**) CCP with a good 68% yield.

3.2. X-ray Structure Study

Compounds **1–6** comprise virtually identical $\{\text{Mn}^{\text{II}}_4\text{Mn}^{\text{III}}_2\text{O}_2\}^{10+}$ cores consisting of two edge-shared distorted Mn_4 tetrahedra with two $\mu_4\text{-O}^{2-}$ ions lying inside of each tetrahedron and which are similar to the earlier described compounds [1–9]. The common edge is formed by two Mn^{III} ions with the shortest intracluster $\text{Mn}\cdots\text{Mn}$ distance being 2.812(2)–2.824(1) Å. All other $\text{Mn}^{\text{III}}\cdots\text{Mn}^{\text{II}}$ and $\text{Mn}^{\text{II}}\cdots\text{Mn}^{\text{II}}$ bond distances in Mn_4 tetrahedra are longer (~3.2 and 3.7 Å, respectively). Peripheral ligation is provided by 10 bridging pivalate (**1**, **2**, **3**, **6**) or isobutyrate (**4**, **5**) monoanionic ligands, six of them coordinated in a μ_2 -mode and four other in a μ_3 -mode. All Mn^{II} atoms have a near-octahedral surrounding. The Mn^{III} ions (Mn1 and Mn2) have an elongated octahedral MnO_6 environment. The values of axial and equatorial $\text{Mn}^{\text{III}}\text{--O}$ bond lengths are in the range 2.211(2)–2.275(5) and 1.883(4)–1.978(2) Å, respectively. Selected bond lengths are summarized in Table S1. Four peripheral Mn atoms are in the lower oxidation state 2+ and have longer $\text{Mn}\text{--O}_{\text{carb.}}$ bond distances ranging from 2.091(4) to 2.399(2) Å. Oxygen atoms of bridging pivalate or isobutyrate ligands and $\mu_4\text{-O}$ atoms occupy only five vertices in each Mn^{II} coordination octahedron, and their sixth position is occupied by terminally capped or bridged ligands. The nature and mutual arrangement of these capped and/or bridging ligands determine the manner of intercluster supramolecular interactions and ultimately the crystal structure architecture.

In compounds **1–3**, the coordination surrounding of the Mn^{II} atoms is completed by monodentate carboxylate and solvate molecules and results in discrete clusters. In the crystals of **1** and **2**, the clusters are aggregated exclusively via hydrophobic-lipophilic interactions, while in **3**, the clusters additionally interact through intermolecular hydrogen bonds involving solvent molecules. In **1**, the sixth position in the Mn3 octahedron is occupied by an ethanol molecule with $\text{Mn}\text{--O}$ bond distance of 2.217(2) Å, while other peripheral Mn4, Mn5 and Mn6 atoms are capped by oxygen atoms of the pivalic acid molecules ($\text{Mn}\text{--O}$ bond distances are equal to 2.233(2), 2.226(2) and 2.207(2) Å, respectively), Figure 1a. The orientation of these pivalic acid molecules is stabilized by strong intramolecular $\text{O}\cdots\text{H}\cdots\text{O}$ hydrogen bonds with the neighboring bridging pivalate ligand ($\text{O}\cdots\text{H}\cdots\text{O}$ is equal 2.567(2), 2.584(2) and 2.667(2) Å). The solvate pivalic acid molecule associates via two $\text{O}\cdots\text{H}\cdots\text{O}$ hydrogen bonds with the $\{\text{Mn}_6\}$ cluster and results in a completely closed hydrophobic exterior shell of the cluster (Figure 1b).

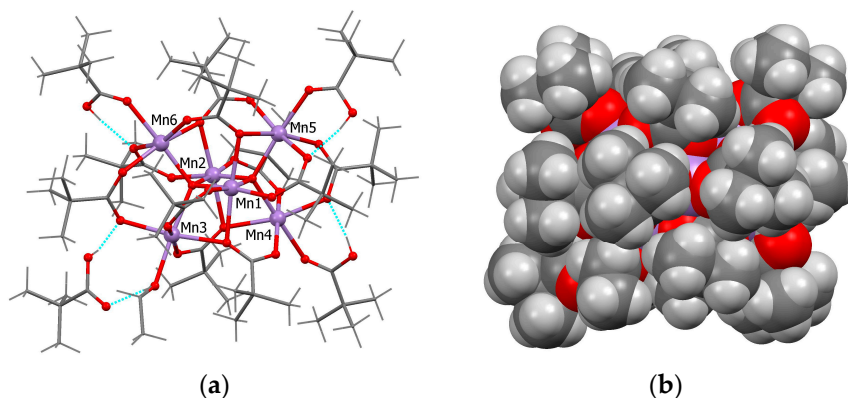


Figure 1. (a) View of the cluster and H-bonded pivalic acid molecule in **1**; (b) Space-filling model of the H-bonded associate illustrates the hydrophobic exterior shell of the cluster.

In crystal structure **2**, $\{Mn_6\}$ cluster resides on two-fold axis passing through both μ_4 -O atoms, thus presuming C_2 molecular symmetry of the cluster and only three Mn atoms are symmetry independent. However, it should be noted, that two-fold axis is passed also through two pivalate ligands, which bridge symmetry related Mn2, Mn2' and Mn3 and Mn3' atoms (Figure 2a). The pivalate ligands do not possess the two-fold symmetry due to the presence of *tert*-butyl group and that implies the disorder of *tert*-butyl groups over two positions due to the crystal symmetry. This disorder also introduces the disorder in positions of both two pivalic acid molecules which cap the Mn3 and Mn3' atoms and solvent ethanol molecules associated with the cluster via H-bonds.

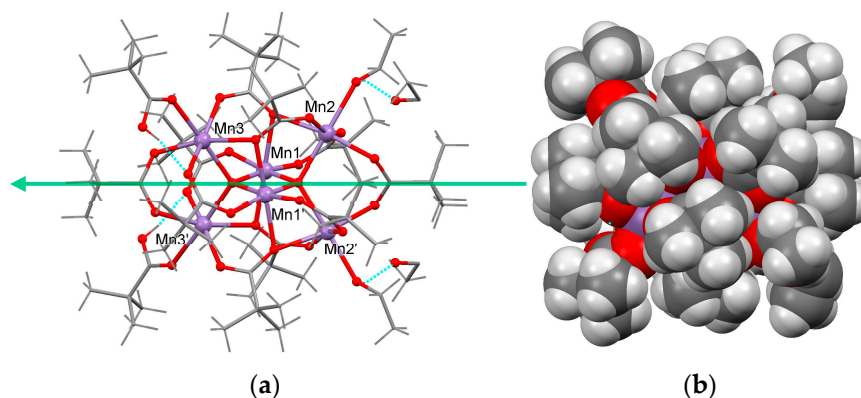


Figure 2. (a) View of the cluster and H-bonded ethanol molecules in **2**. The green arrow shows the two-fold rotation axis passing through the cluster in the crystal structure. (b) Space-filling model. The second positions of disordered moieties are not shown.

In **2**, two symmetry related peripheral Mn atoms (Mn2 and Mn2') in the Mn_4 tetrahedra are capped by ethanol molecules. Two peripheral Mn atoms in the second Mn_4 tetrahedra (Mn3 and Mn3') are capped by disordered molecules of pivalic acid. Similar to **1**, the positions of these disordered molecules are stabilized by intramolecular O–H...O bonds, Table S2. The disordered solvate ethanol molecule is hydrogen bonded with the cluster via coordinated ethanol molecules and similar to **1**, closes the hydrophobic shell of the cluster (Figure 2b).

In **3**, the *tert*-butyl group of three bridging pivalate ligands and one methanol solvent molecule were found to be disordered over two positions. The sixth position in the Mn^{II} atoms environment in each Mn_4 tetrahedron is filled by coordinated pivalic acid or methanol molecules. Thus, the mutual arrangement of pivalic acid/alcohol molecules that cap peripheral Mn^{II} atoms differs from their arrangement in cluster **2**, (Figure 3a). Similar to **1** and **2**, each of the pivalic acid molecules forms strong intramolecular hydrogen bonds (2.587(3) and 2.630(5) Å), which stabilize their orientation. The peculiarity of this cluster is related with solvent water molecules attached to the cluster by two O–H...O hydrogen bonds (2.882(3) and 2.838(4) Å). The lone pairs of this interstitial water molecule are pointing outside the cluster and create the hydrophilic region on the cluster surface predisposed for an involvement in hydrogen bonds, (Figure 3b). The solvent methanol molecules are H-bonded with water molecules (O–H...O = 2.691(4) Å) forming water-methanol solvent molecule associates and are also involved in the hydrogen bonds with coordinated methanol molecules of neighboring clusters (O–H...O = 2.642(4) Å). As a result, clusters are joined in zigzag-like H-bonded polymeric chains extended along the *b* crystallographic axis, (Figure 3c). The second symmetry independent methanol molecule is disordered over two positions and H-bonded to another coordinated methanol molecule in the cluster, thus it decorates the chain (O–H...O = 2.63(1)/2.74(2) Å).

In the crystal structure **4**, the peripheral ligation of metal atoms is provided by 10 bridging isobutyrate ligands instead of pivalate ones in **1–3**. Three isobutyrate ligands revealed disorder of the isopropyl group over two positions. Two methanol molecules *trans*-positioned across the cluster center and two pyrazine ligands *trans*-positioned and symmetry related by translation *b* cap the Mn^{II} atoms.

The bridging exo-bidentate pyrazine molecules link $\{Mn_6\}$ cluster moieties into linear coordination polymers which propagate along the crystallographic b axis (Figure 4).

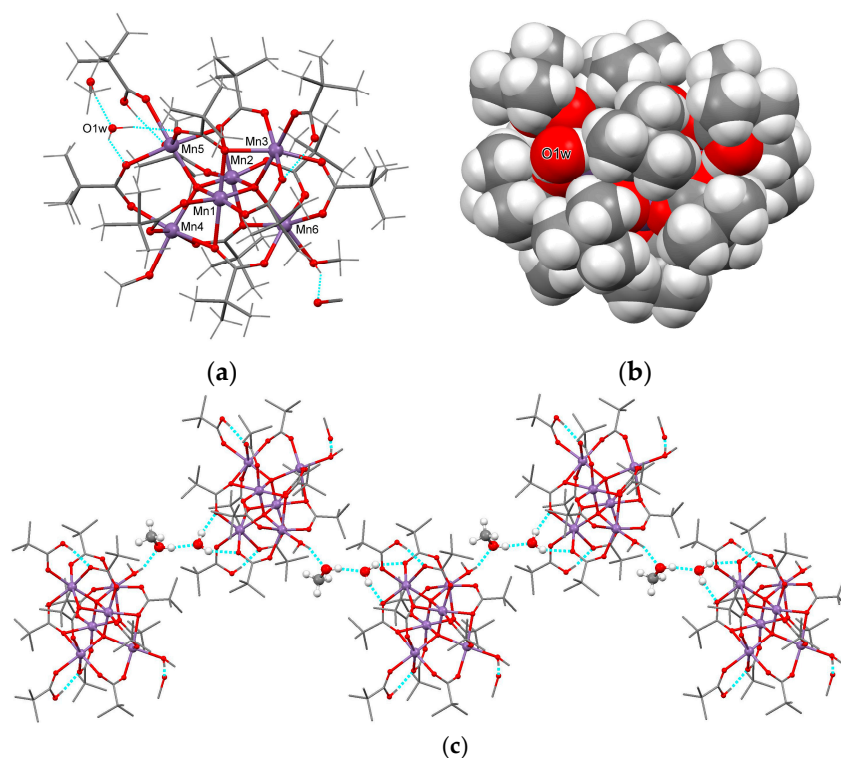


Figure 3. (a) View of the formula unit of **3**. The second position of the disordered groups/molecules is not shown. (b) Space-filling model illustrates the position of the interstitial solvent water molecule on the cluster surface. (c) Zigzag-like H-bonded polymeric chain of clusters. The water-methanol H-bonded associates are highlighted by bigger radii balls.

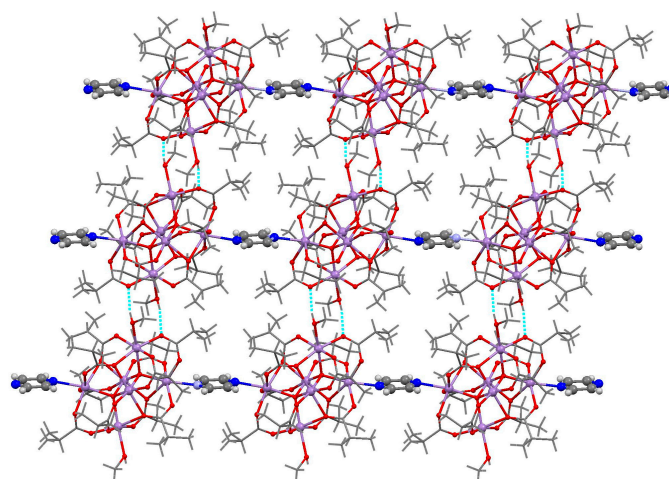


Figure 4. The fragment of the structure of **4** illustrates the incorporation of $\{Mn_6\}$ clusters into the 1D linear coordination polymer and hydrogen bonding of parallel polymeric chains into a layer. The bridging pyrazine molecules are shown by bigger radii balls.

The intercluster $Mn \cdots Mn$ separation through the pyrazine molecule is equal to 7.443(2) Å. This distance is slightly longer than the corresponding distance of 7.288(3) Å in the related zigzag-like

coordination polymer of composition $\{[\text{Mn}_6\text{O}_2(\text{O}_2\text{CCHMe}_2)_{10}(\text{pyz})_3]\cdot 2\text{H}_2\text{O}\}_n$ [5], where unlike **4**, bridging pyrazine molecules are *cis*-situated and attached to Mn^{II} atoms of the same Mn_4 tetrahedron of the cluster. The adjacent, inversion symmetry related parallel polymeric chains, are connected via $\text{O}\cdots\text{H}\cdots\text{O}$ (2.739(7) and 2.721(7) Å) hydrogen bonds between methanol molecules and pivalate ligands, which results in a supramolecular layer parallel to the $(-1\ 0\ 1)$ plane. The shortest interchains $\text{Mn}\cdots\text{Mn}$ distances between H-bonded clusters in the layer are equal to 5.496(1) and 5.454(1) Å. Parallel layers are stacked exclusively via hydrophobic-lipophilic interactions.

In **5** with composition $\{[\text{Mn}_6\text{O}_2(\text{O}_2\text{CCHMe}_2)_{10}(\text{pyz})_{1.5}(\text{H}_2\text{O})]\cdot 0.5(\text{H}_2\text{O})\}_n$, the sixth coordination sites of four Mn^{II} ions in the $\{\text{Mn}_6\}$ cluster are occupied by three bridging pyrazine ligands and one water molecule. Thus, these clusters may be considered as T-shaped connectors from the view point of an extended coordination polymer structure development. The pyrazine molecules bind clusters which are symmetry related by translation b ($\text{Mn}\cdots\text{Mn} = 7.415(1)$ Å), similar to the linear coordination chain in **4**. Another symmetry independent pyrazine molecule connects neighboring clusters in a well-defined ladder-like structure (Figure 5). The interchain $\text{Mn}\cdots\text{Mn}$ bond distance through the pyrazine bridge is equal to 7.480(1) Å. The chains are interrelated by $\text{O}\cdots\text{H}\cdots\text{O}$ hydrogen bonds involving the coordinated and solvent H_2O molecules (2.713(6) Å) and solvent water molecules and isobutyrate ligands (2.742(5) and 2.899(6) Å) (Table S2), which results in supramolecular layers parallel to the $[-1\ 0\ 1]$ crystallographic plane. The shortest $\text{Mn}\cdots\text{Mn}$ separation between H-bonded clusters of neighboring ladder-like chains in the layer is equal to 5.336(1) Å. Similar to **4**, the parallel layers are stacked exclusively via hydrophobic-lipophilic interactions.

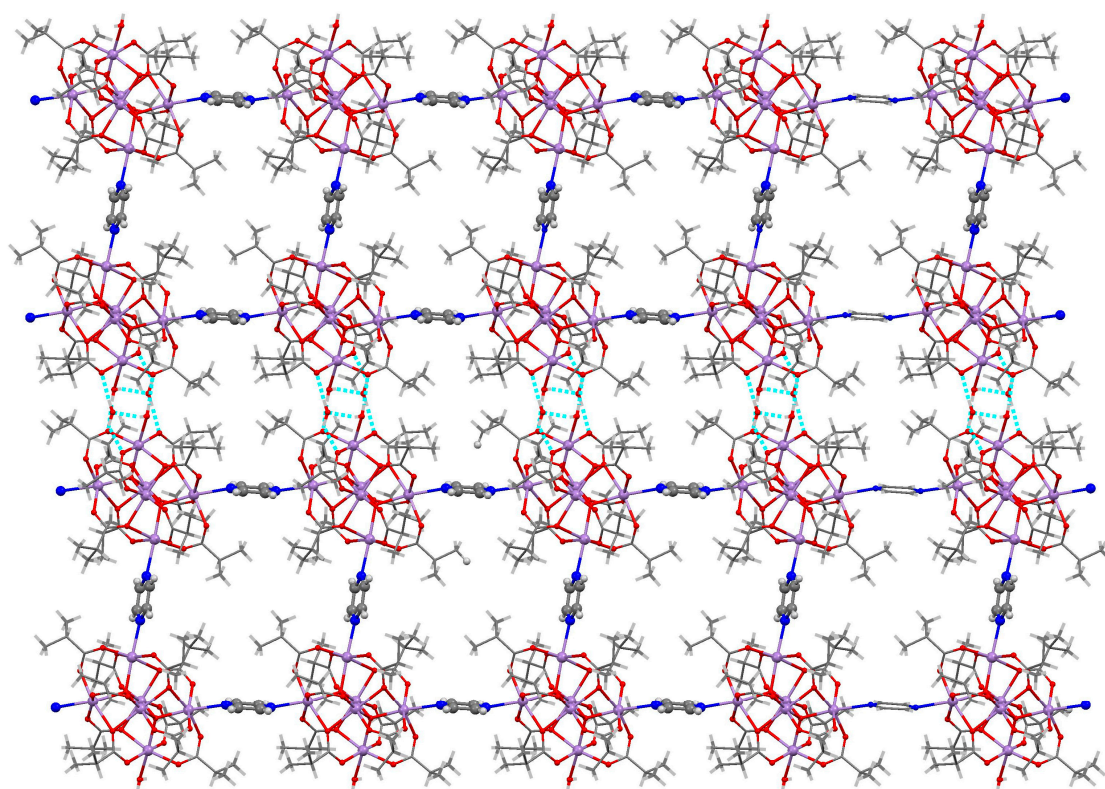


Figure 5. View of the ladder-like 1D coordination polymer of **5**, hydrogen bonded into a supramolecular layer. The bridging pyrazine molecules are shown by bigger radii balls.

In the 1D coordination polymer $[\text{Mn}_6\text{O}_2(\text{O}_2\text{CCMe}_3)_{10}(\text{Me}_3\text{CCO}_2\text{H})_2(\text{en})]_n$ (**6**), shown in Figure 6, pivalic acid molecules cap the terminal *trans*-positioned Mn^{II} sites, which belong to different Mn_4O tetrahedra. One of the pivalic acid molecules and *tert*-butyl groups of two pivalate ligands are disordered over two positions. The positions of pivalic acid molecules are stabilized by intramolecular

O–H···O hydrogen bonds (2.56(1), 2.61(2), and 2.84(2) Å). The ethyl nicotinate (en) O,N-ligands coordinate via the pyridine nitrogen atom to the *trans*-positioned Mn^{II} atoms (Mn–N = 2.314(5) Å) and via the oxygen atom of the ethyl ester group (Mn–O = 2.298(5) Å) and unite {Mn₆} clusters into 1D coordination polymers. The intracuster Mn···Mn distance in the chain through the en spacer ligand is 8.527(1) Å. The chains run along the [1 0 1] direction and are packed parallel to each other in the lattice.

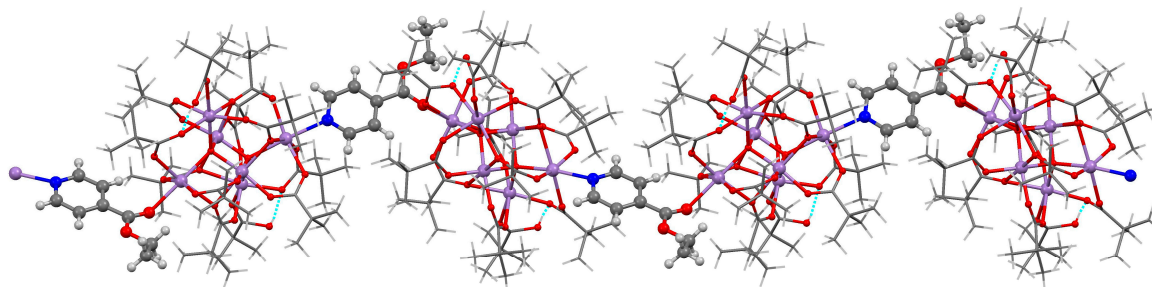


Figure 6. View of a 1D coordination polymer in **6**. The bridging ethyl nicotinate molecules are shown by bigger radii balls.

The crystal structures of **1–6** reveal a close packing motif, mostly due to hydrophobic-lipophilic interactions. Upon removing solvent molecules and disordered fragments/molecules of the second positions, the total solvent-accessible volume obtained using PLATON [14] was estimated to be only 10.7% in **1**, 13.8% in **2**, 5.0% in **3**, 4.4% in **4**, 4.9% in **5** and 1.4% in **6**.

4. Conclusions

Based on the crystal structure of six new compounds, we demonstrated how the nanosized hexanuclear mixed-valent carboxylate manganese coordination clusters with a hydrophobic surface may be incorporated in hydrogen bonded or polymeric supramolecular extended structures through the modification of the cluster surface by a diverse combination of capping or bridging ligands attached to peripheral Mn atoms. In contrast to the secondary building unit (SBU) approach, we use cluster as supermolecular building block (SBB) [15] which may be isolated to produce the supramolecular extended structure without risking cluster decomposition or rearrangement. The relative size of coordination clusters vs. metal ions may afford unprecedented advances in terms of scale to develop extended supramolecular structures.

Supplementary Materials: The following are available online at www.mdpi.com/2073-4352/8/2/100/s1, Figure S1: View of clusters **1–3** illustrates the diverse combination of capped ligands attached to peripheral Mn^{II} atoms. CIF files of the solved structure. Table S1: Selected bond distances (Å) in **1–6**, Table S2: The parameters of O–H···O hydrogen bonds in the crystal structure **1–6**.

Acknowledgments: This study was supported by the project CSSDT 15.817.02.06F and the Swiss National Science Foundation (SCOPES IZ73Z0_152404/1).

Author Contributions: Mariana Darii and Svetlana Baca conceived and designed the experiments; Mariana Darii performed the synthetic experiments; Jürg Hauser and Victor Kravtsov performed the X-ray measurements; Irina Filippova and Victor Kravtsov analyzed the data; all authors took part in writing and discussion of the paper.

Conflicts of Interest: The authors declare no conflict of interest.

References

1. Baca, S.G. The design of coordination networks from polynuclear Mn(II, III) and Fe(III) oxo-carboxylate clusters. In *Advances in Chemistry Research*; Taylor, J.C., Ed.; Nova Science Publishers, Inc.: New York, NY, USA, 2018; Volume 43, ISBN 978-1-53613-079-9.
2. Nakata, K.; Miyasaka, H.; Sugimoto, K.; Ishii, T.; Sugiura, K.; Yamashita, M. Construction of a one-dimensional chain composed of Mn₆ clusters and 4,4'-bipyridine linkers: The first step for creation of “nano-dots-wires”. *Chem. Lett.* **2002**, *31*, 658–659. [[CrossRef](#)]

3. Moushi, E.E.; Tasiopoulos, A.J.; Manos, M.J. Synthesis and structural characterization of a metal cluster and a coordination polymer based on the $[\text{Mn}_6(\mu_4\text{-O})_2]^{10+}$ unit. *Bioinorg. Chem. Appl.* **2010**, 367128. [[CrossRef](#)] [[PubMed](#)]
4. Ma, C.-B.; Hu, M.-Q.; Chen, H.; Chen, C.-N.; Liu, Q.-T. Aggregation of hexanuclear, mixed-valence manganese oxide clusters linked by propionato ligands to form a one-dimensional polymer $[\text{Mn}_6\text{O}_2(\text{O}_2\text{Cet})_{10}(\text{H}_2\text{O}_4)]_n$. *Eur. J. Inorg. Chem.* **2008**, 5274–5280. [[CrossRef](#)]
5. Malaestean, I.L.; Kravtsov, V.C.; Speldrich, M.; Dulcevscaia, G.; Simonov, Y.A.; Lipkowski, J.; Ellern, A.; Baca, S.G.; Kögerler, P. One-dimensional coordination polymers from hexanuclear manganese carboxylate clusters featuring a $\{\text{Mn}^{\text{II}}_4\text{Mn}^{\text{III}}_2(\mu_4\text{-O})_2\}$ core and spacer linkers. *Inorg. Chem.* **2010**, 49, 7764–7772. [[CrossRef](#)] [[PubMed](#)]
6. Ovcharenko, V.; Fursova, E.; Romanenko, G.; Ikorskii, V. Synthesis and structure of heterospin compounds based on the $[\text{Mn}_6\text{O}_2\text{piv}_{10}]$ -cluster unit and nitroxide. *Inorg. Chem.* **2004**, 43, 3332–3334. [[CrossRef](#)] [[PubMed](#)]
7. Fursova, E.Y.; Ovcharenko, V.I.; Bogomyakov, A.S.; Romanenko, G.V. Structure of the complex of hexanuclear manganese pivalate with isonicotinamide. *J. Struct. Chem.* **2013**, 54, 164–167. [[CrossRef](#)]
8. Malaestean, I.L.; Ellern, A.; van Leusen, J.; Kravtsov, V.C.; Kögerler, P.; Baca, S.G. Cluster-based networks: Assembly of a (4,4) layer and a rare T-shaped bilayer from $[\text{Mn}^{\text{III}}_2\text{Mn}^{\text{II}}_4\text{O}_2(\text{RCOO})_{10}]$ coordination clusters. *CrystEngComm* **2014**, 16, 6523–6525. [[CrossRef](#)]
9. Kar, P.; Halder, R.; Gómez-García, C.J.; Ghosh, A. Antiferromagnetic porous metal-organic framework containing mixed-valence $[\text{Mn}^{\text{II}}_4\text{Mn}^{\text{III}}_2(\mu_4\text{-O})_2]^{10+}$ units with catecholase activity and selective gas adsorption. *Inorg. Chem.* **2012**, 51, 4265–4273. [[CrossRef](#)] [[PubMed](#)]
10. Baca, S.G.; Clerac, R.; Sevryugina, Y.; Malaestean, I.; Gerbelev, N.; Petrukhina, M.A. Linear trinuclear manganese(II) complexes: Crystal structures and magnetic properties. *Inorg. Chem. Commun.* **2005**, 8, 474–478. [[CrossRef](#)]
11. Baca, S.G.; Malaestean, I.L.; Keene, T.D.; Adams, H.; Ward, M.D.; Hauser, J.; Neels, A.; Decurtins, S. One-dimensional manganese coordination polymers composed of polynuclear cluster blocks and polypyridyl linkers: Structures and properties. *Inorg. Chem.* **2008**, 47, 11108–11119. [[CrossRef](#)] [[PubMed](#)]
12. Murrie, M.; Parsons, S.; Winpenny, R.E.P. Deltahedra as underlying structural motifs in polynuclear metal chemistry: Structure of an undecanuclear manganese-potassium cage. *J. Chem. Soc. Dalton Trans.* **1998**, 9, 1423–1424. [[CrossRef](#)]
13. Sheldrick, G.M. A short history of SHELX. *Acta Crystallogr.* **2008**, A64, 112–122. [[CrossRef](#)] [[PubMed](#)]
14. Spek, A.L. Single-crystal structure validation with the program PLATON. *J. Appl. Crystallogr.* **2003**, 36, 7–13. [[CrossRef](#)]
15. Cairns, A.J.; Perman, J.A.; Wojtas, L.; Kravtsov, V.C.; Alkordi, M.H.; Eddaoudi, M.; Zaworotko, M.J. Supramolecular building blocks (sbbs) and crystal design: 12-connected open frameworks based on a molecular cubohemioctahedron. *J. Am. Chem. Soc.* **2008**, 130, 1560–1561. [[CrossRef](#)] [[PubMed](#)]

